CRACK GROWTH IN MASSIVE FORMING: A FRACTURE MECHANICS APPROACH

Gernot Trattnig[1,a], Christof Sommitsch[2,b], Reinhard Pippan[1,c]
[1)] Erich Schmid Institute of the Austrian Academy of Sciences, Leoben, Austria
Christian Doppler Laboratory for local Analysis of Deformation and Fracture
[2)] Böhler Edelstahl GmbH, Kapfenberg, Austria
[a)]trattnig@unileoben.ac.at, [b)]christof.sommitsch@bohler-edelstahl.at,
[c)]pippan@unileoben.ac.at

Abstract

The appearance of cracks is of major importance in massive forming processes. In order to avoid failure of workpieces it is important to understand the dependence of crack growth on the initial flaw size and the stress state. This work examines this relationship with different specimen geometries and testing methods at ambient temperature. Beside standard fracture mechanics experiments to determine the J-Integral and the crack tip opening displacement of steel X5NiCrTi26-15 (Böhler T200) tension and compression tests on pre-cracked samples with different crack lengths were carried out. The compression experiments were conducted with split cylindrical specimens with pre-cracks parallel to the compression axis which permits the observation of crack opening displacement as a function of crack extension inside the specimen.

It was shown that the crack opening displacement (COD) in deeply cracked tension specimens decreased to half the value of shallow cracked specimens, and that the critical COD values for pre-cracked compression specimens were in the same order like of tension samples with short surface cracks.

Introduction

Crack initiation and crack growth are of major importance in production processes like forming. It is known that the crack resistance depends on the stress triaxiality. Matsoukas *et al.* [1] showed for example that short surface cracks with low stress triaxiality have a significant higher critical COD than deep cracks with high stress triaxiality.

Massive forming workpieces generate highly different loading modes and stress states compared to usual mechanical loading or standard fracture mechanics specimens used for determining the fracture toughness, e.g. BS 5762 [2], E 1290-89 [3]. By choosing different specimen geometries and crack depths, large differences in stress triaxiality were achieved and their influence on the fracture toughness was investigated. The specimen geometries should reproduce typical failure types in massive forming, like vertical cracks in cylindrical upsetting samples.

Experiments

Used Material

All experiments were carried out with the austenic steel X5NiCrTi26-15 (Böhler T200). This steel is used e.g. in aviation industry or as turbine blade material. The 0.2 % offset yield

strength (σ_{yield}) of the used steel as received is 750 MPa and the tensile strength is about 1280 MPa.

The specimens were prepared from a rod with a diameter of 60 mm in a way that the crack always propagated in the C-R direction (following ASTM notation, Anderson [4]). All examined fracture surfaces had this orientation in order to exclude anisotropy effects. Experiments were carried out at room temperature.

Determination of Crack Opening Displacement (COD) versus Crack Propagation

The COD versus crack propagation curves for the different specimens are achieved from stereoscopic scanning electron microscope (SEM) images of the fractured surface, by using the technique of Scherer and Kolednik [5] and Scherer *et al.* [6], respectively.

The procedure to gain the COD versus crack propagation curves is explained exemplarily on the basis of the obtained fracture surfaces of a cylindrical tension specimen with a 0.4 mm deep circumferential crack. Fig. 1 shows two corresponding fracture surfaces of this tension specimen after rupture under tensile load.

The strong texture alignment of voids in rolling direction can be clearly seen in Fig. 2. Corresponding paths are marked in the images of the fracture surfaces (Fig. 1). Along these lines two height profiles are extracted from the three dimensional fracture surface data (Fig. 2). These gained height profiles are shown in Fig. 3.

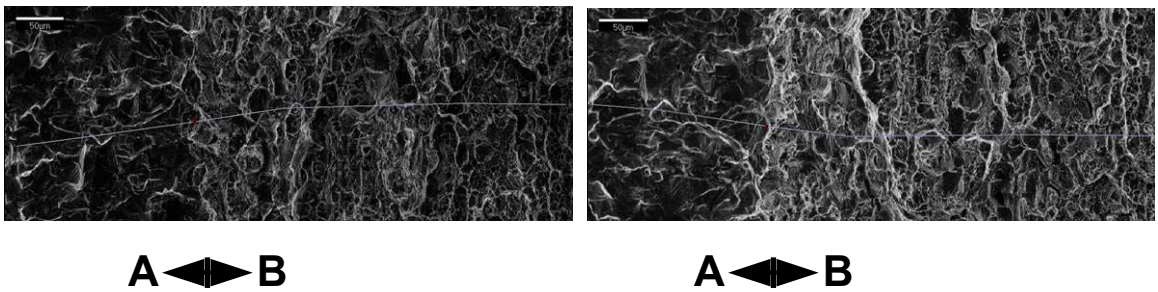

FIGURE 1. SEM images of the corresponding fracture surfaces with the crack propagation direction from left to right (A ... fatigue pre-crack, B ... overload fracture).

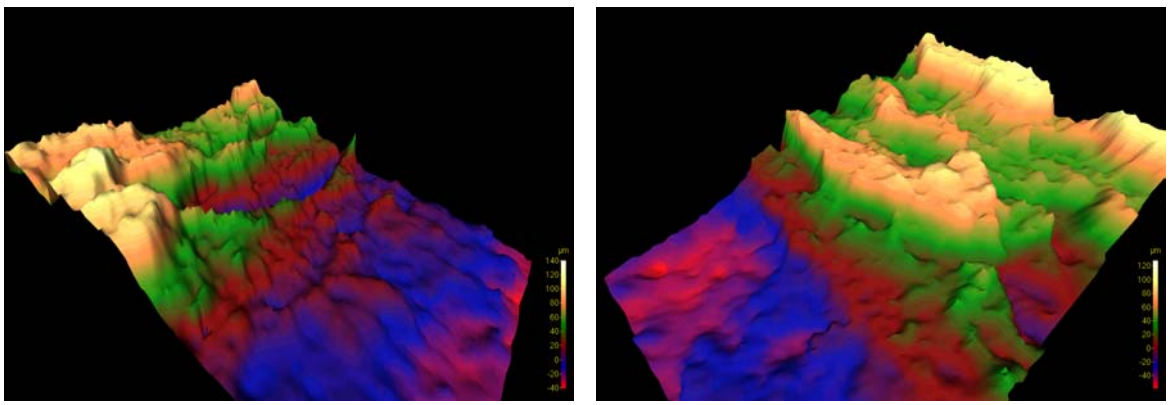

FIGURE 2. Stereoscopic SEM images of corresponding fracture surfaces from a cylindrical tension specimen with a 0.4 mm deep circumferential crack.

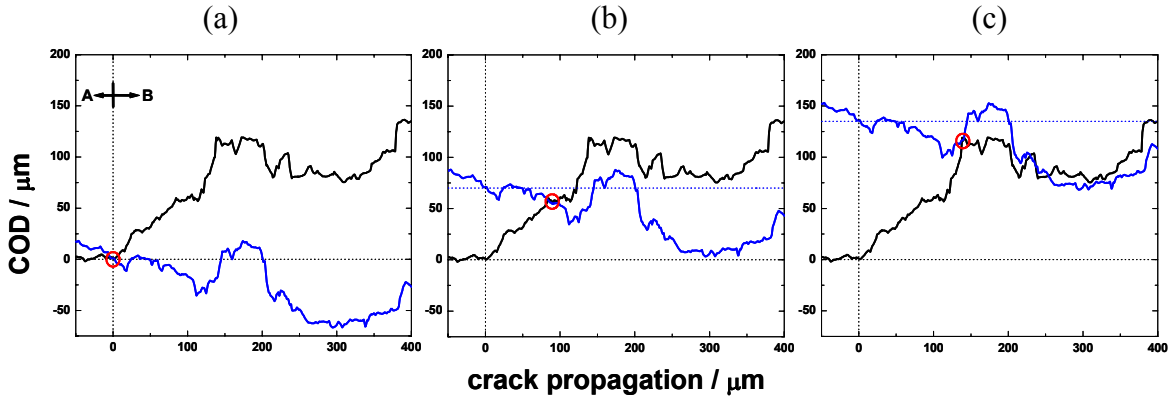

FIGURE 3. Vertical shift of the upper fracture profile (blue) versus the lower fracture profile (black) in order to achieve a single COD versus crack propagation curve.

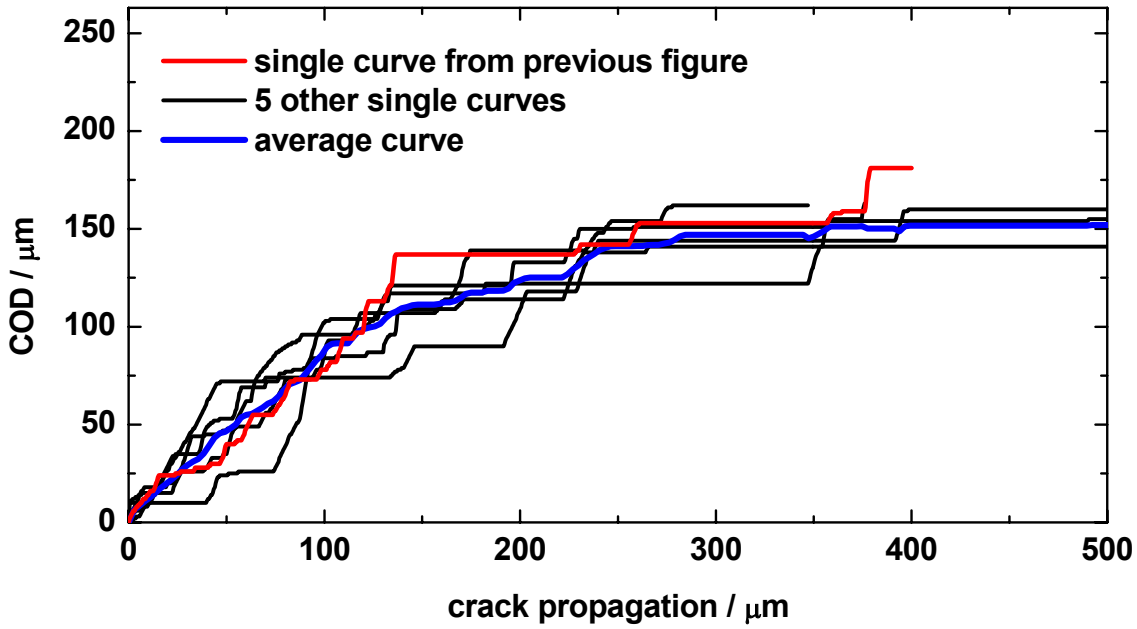

FIGURE 4. Averaged COD versus crack propagation curve out of 6 single curves from the 0.4 mm deep cracked cylindrical tension sample.

The black curve in Fig. 3 represents the height profile in the lower fracture surface, the blue one the height profile in the upper surface. By shifting the lower profile vertical a single COD versus crack propagation curve is obtained, because the vertical transition of the upper profile corresponds to the COD and the x-coordinate of the front intersection point of the two profiles represents the crack extension.

Fig. 3.a shows the situation after fatigue cracking and before overload rupture by tensile loading occurs. The crack propagation is zero, marked by a red circle. In Fig. 3.b the profile from the upper surface is shifted by 70 µm, which represents the COD value, and the front intersection point is at a crack extension of 90 µm, again marked by a red circle. In Fig. 3.c the COD value is 135 µm at a crack extension of 138 µm. In this way a single COD versus crack propagation curve is achieved (red curve in Fig. 4).

On one measurement point of the fracture surface several single COD versus crack propagation curves are obtained (black curves in Fig. 5). The average of these single curves is the resulting curve for this 0.4 mm deep cracked cylindrical tension specimen (blue average

curve in Fig. 4). All COD versus crack propagation curves for cylindrical tension samples and the CT specimen are obtained in this way (Fig. 7).

Compact Tension (CT) Specimen

The used CT specimen had a width (W) of 32 mm and 2 mm deep side grooves. The crack propagation was measured with the direct-current-potential-drop method (DCPM), Riemelmoser *et al.* [7]. The test agreed with the ASTM E-813-89$^{\varepsilon 1}$ [8] standard, so the derived J_Q value of 61.8 kJm^{-2} (Fig. 5) is equal to J_{IC}. The measured blunting line deviates from the theoretical blunting line. This can be attributed to the overestimation of the crack propagation by DCPM caused by the plastic deformation of the specimen [7]. The blunting region was not corrected for the J_{IC} determination.

The CT specimen has the highest stress triaxiality, so the COD versus crack propagation curve can be used as a reference to compare it with the curves obtained from the cylindrical tension specimens (Fig. 7). The critical COD value, gained from stereoscopic SEM images, is about 60 μm. From this a J_{IC} value of about 110 kJ/m^{-2} is expected ($J = COD.\sigma_{yield}.m$, m...material constant) the difference may be caused by the overestimation of the crack propagation by DCPM.

Cylindrical Tension Specimens

In order to study the influence of the crack depth on the crack growth cylindrical tension specimens with sharp circumferential notches (Fig. 6) were tested.

Fatigue cracks were introduced by cyclic compressive and tensile loading. The fatigue cracks had a depth, measured from the notch root, of about 0.3 mm. After that the effective sample diameter X was reduced to 22.0, 16.6, 12.0, 11.3, and 10.9 mm to obtain the different crack depths 5.7, 3.1, 0.7, 0.4, and 0.2 mm, respectively. In this way it was possible to examine samples with different stress triaxiality at the crack tip. The remaining cross section was the same for all specimens.

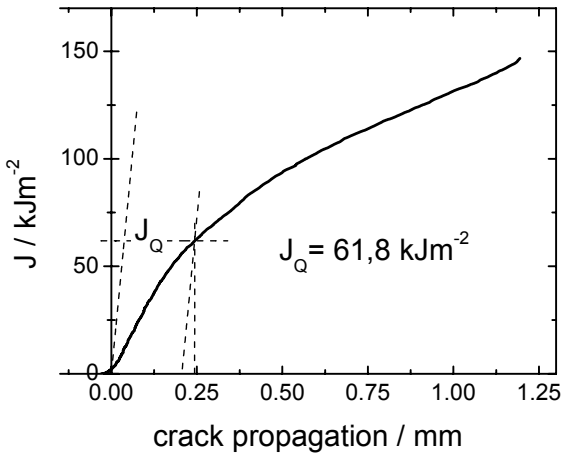

FIGURE 5. J Integral versus crack propagation for steel X5NiCrTi26-15, measured on a side grooved CT specimen (width W = 32 mm).

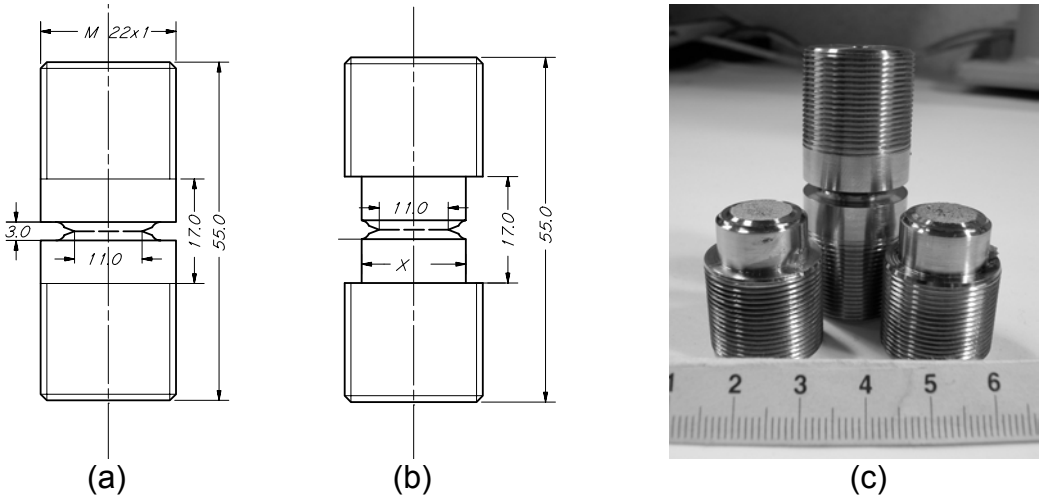

FIGURE 6. Sketch of the specimens to introduce the fatigue crack (a); to realize different crack depths the effective diameter (X) of the fatigue pre-cracked specimens was reduced to values between 22.0 and 10.9 mm (b); (c) shows a specimen for pre-cracking and two halves of a ruptured specimen with a finale sample diameter of 16.6 mm.

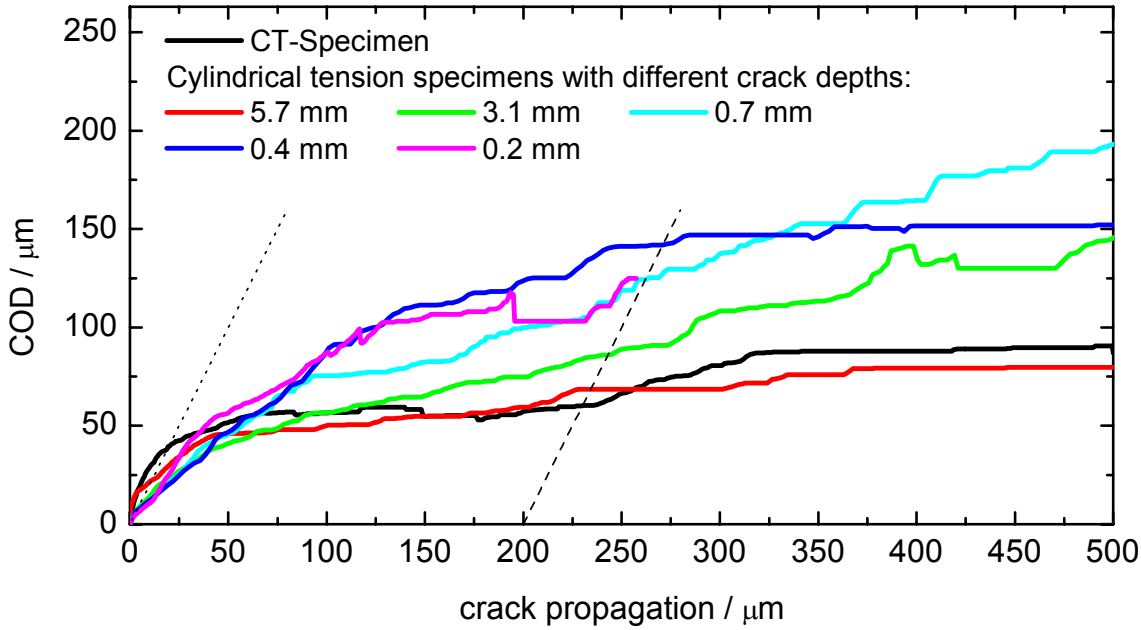

FIGURE 7. COD versus crack propagation of the CT and the cylindrical tension specimens.

The specimens were loaded until rupture with a standard tensile testing machine. The required force for the specimen with 5.7 mm crack depth and high stress triaxiality was 135 kN, for the specimen with 0.4 mm crack depth and low stress triaxiality just 85 kN. This large difference demonstrates the large variation in the stress triaxiality. The COD versus crack propagation curves were obtained by the previously described technique. The results for the different samples are shown in Fig. 7.

Rice [9] suggested to determine the COD value as the displacement at the intersections of a 90° vertex with the crack flanks. This value corresponds to the intersection of the dotted line with the data curves in Fig. 7. Because of the shape of the crack tips in cylindrical tension samples, this line touches the COD versus crack propagation curves tangentially. In

order to get a distinctive value, this line was shifted to a crack propagation of 0.2 mm (dashed line in Fig. 7). Hence the COD value becomes independent on the crack tip geometry and is called $COD_{Rice0.2}$.

Table 1 shows that $COD_{Rice0.2}$ decreases with increasing crack depth and therefore higher stress triaxiality .This is in accordance to results of Motsoukas *et al.* [1].

TABLE 1. Dependence of $COD_{Rice0.2}$ on the crack depth.

crack depth / mm	17 (CT)	5.7	3.1	0.7	0.4	0.2
$COD_{Rice0.2}$ / µm	60	70	85	125	140	125

Cylindrical Upsetting Specimens

A standard experiment in massive forming is the upsetting of cylindrical specimens. To examine the crack growth in this geometry a vertical pre-crack was introduced in such a sample by manufacturing the upsetting specimen from a standard pre-fatigued single edge notched bend (SENB) specimen. This production procedure is sketched in Fig. 8.

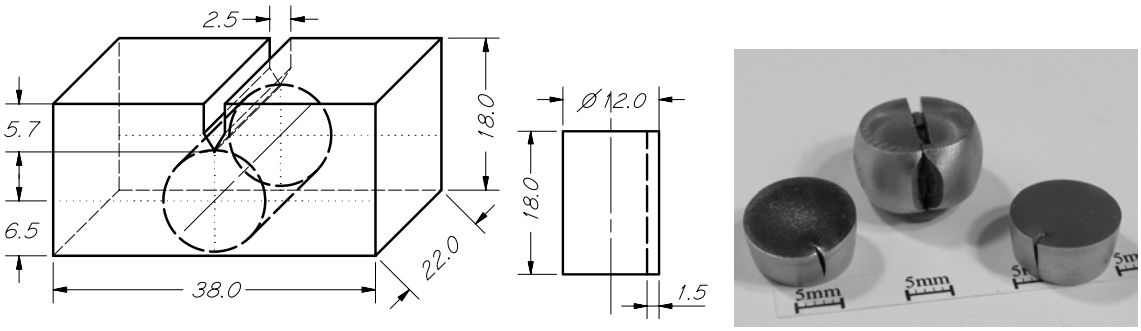

(a) (b) (c)

FIGURE 8. Sketched procedure to manufacture a cylindrical upsetting specimen with a vertical pre-crack (b) from a SENB specimen (a); (c) shows a compressed specimen and two halves of a split sample.

A tested sample, which was compressed to half of its original height, is shown in the center of Fig. 8.c. The contact surfaces of the sample and the upsetting dies were sandblast to gain high friction, and thereby strong bulging. The upsetting process leads to a growth of the pre-crack. The crack growth is highest in the center of the sample because there are the highest circumferential stresses. After the compression the sample was split vertical and the fracture surfaces were examined by stereoscopic SEM images. In this way it was possible to analyse the final state of the crack but not to gain information about the crack initiation and crack growth, due to the vertical plastic deformation of the wake of the crack.

In order to gain such information with a single specimen technique the prepared cylindrical upsetting samples were cut horizontally in the stress symmetry plane and put together in such a way that again a continuous crack existed. This split samples were compressed step by step and SEM images of the cracks were taken for each step. The compression lead to symmetric growth of the crack in both halves of the samples (Fig. 9) and it was possible to observe blunting, crack initiation and crack growth inside these split samples (Fig. 10).

For a sample with a 1.5 mm deep fatigue crack, shown in Fig. 10, a critical COD about 80 μm was measured. Table 2 shows the measured COD versus crack propagation. It is remarkable that this value for a 1.5 mm deep cracked compression sample is in a comparable range to the $COD_{Rice0.2}$ value for a 1.5 mm deep pre-cracked tension sample, where a value of about 100 μm was estimated.

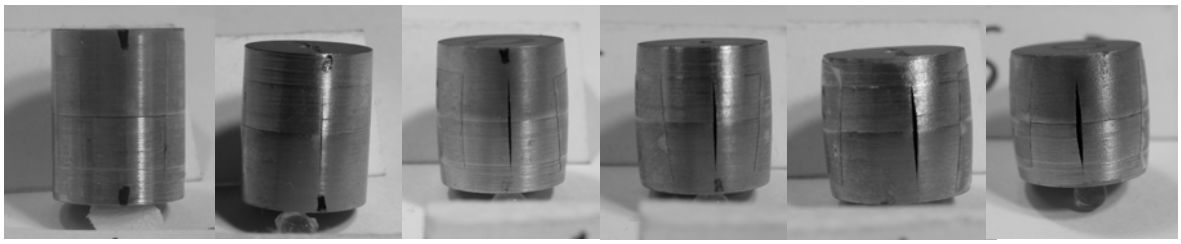

FIGURE 9. Split upsetting sample, stepwise compressed from h_0 = 15.3 mm by Δh = 0.6, 1.0, 0.3, 0.7, and 0.3 mm (from left to right).

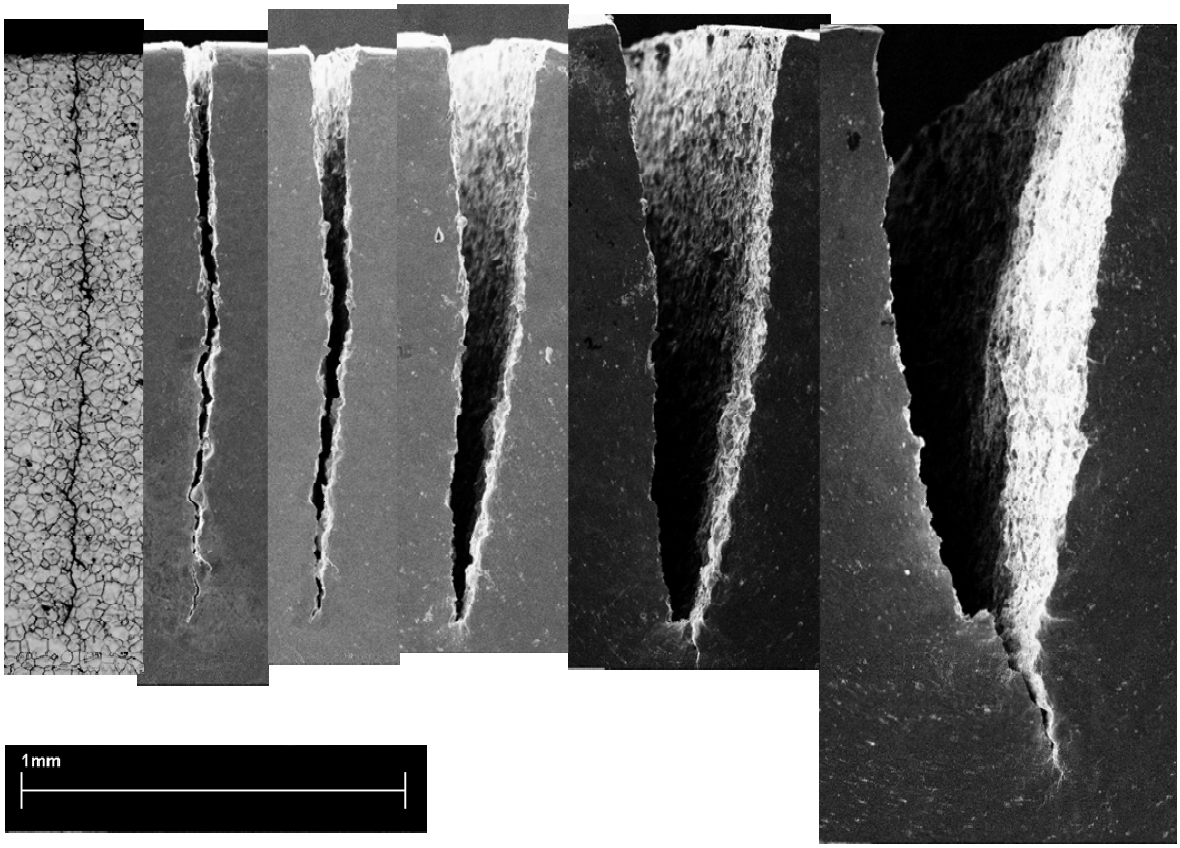

FIGURE 10. Blunting, crack initiation and crack growth in a split cylindrical upsetting specimen with a 1.5 mm deep fatigue crack. Leftmost a light optical micrograph of the non deformed specimen, followed by SEM images of the deformed specimen, upset from h_0 = 17.9 mm by Δh = 1.1, 0.7, 1.1, 1.1, and 0.8 mm.

TABLE 2. COD versus crack propagation from the split upsetting specimen with a 1.5 mm deep fatigue crack.

crack propagation / μm	0	140	435
COD / μm	40	80	235

Conclusion

With stereoscopic SEM images and the presented method to analyse the gained three dimensional fracture surfaces, it is possible to generate accurate COD versus crack propagation plots. The introduced $COD_{Rice0.2}$ is valuable to compare the results achieved by different specimens with large deviations in their stress triaxiality.

It was shown that $COD_{Rice0.2}$ for shallow cracks with low stress triaxiality is twice as high as for the deep cracks with high stress triaxiality (Tab. 1), namely 140 μm for a 0.4 mm shallow crack, compared to 60 μm in the CT specimen.

By the technique of split specimens it is possible to observe blunting, crack initiation and crack growth inside of upsetting samples. The observed critical COD value was between the minimum and maximum value of the tension specimens.

The financial support by the Christian Doppler Laboratory for local Analysis of Deformation and Fracture is acknowledged.

References

1. Matsoukas, G., Cotterell, B. and Mai, Y.-W., *Engineering Fracture Mechanics,* vol. **24**, nr. 6, 837-842, 1986.
2. BS 5762: 1979, *British Standards Institution*, London, UK, 1979.
3. E 1290-89, *American Society for Testing and Materials,* Philadelphia, USA, 1989.
4. Anderson, T.L., *Fracture Mechanics - Fundamentals and Applications,* CRC Press, USA, 1991.
5. Scherer S. and Kolednik, O., *The Americas Microscopy and Analysis*, Issue **70**, 15-17, March 2001.
6. Scherer, S., Werth, P., Pinz, A., Tatschl A. and Kolednik, O., In *Electron Microscopy and Analysis 1999: Proceedings of the Institute of Physics Electron Microscopy and Analysis Group Conference, University of Sheffield, 24-27 August 1999,* edited by C.J. Kiely, 107-110.
7. Riemelmoser, F.O., Pippan, R., Weinhandl, H. and Kolednik O., *Journal of Testing and Evaluation,* vol. **27**, no. 1, 42-46, 1999.
8. E813-89$^{\varepsilon 1}$, *Annual Book of ASTM Standards,* section 3, vol. **03.01**, Philadelphia, USA, 1993.
9. Rice, J.R., *Journal of Applied Mechanics*, vol. **35**, 379-386, 1968.